

Negative Magnetoresistance without Chiral Anomaly in Topological Insulators

Xin Dai,¹ Z. Z. Du,^{2,3} and Hai-Zhou Lu²

¹*Institute for Advanced Study, Tsinghua University, Beijing 100084, China*

²*Institute for Quantum Science and Engineering and Department of Physics, South University of Science and Technology of China, Shenzhen 518055, China*

³*School of Physics, Southeast University, Nanjing 211189, China*

(Dated: September 20, 2022)

An intriguing phenomenon in topological semimetals and topological insulators is the negative magnetoresistance observed when a magnetic field is applied along the current direction. A prevailing understanding to the negative magnetoresistance in topological semimetals is the chiral anomaly, which, however, is not well defined in topological insulators. We calculate the magnetoresistance of a three-dimensional topological insulator, by using the semiclassical equations of motion in which the Berry curvature explicitly induces an anomalous velocity and orbital magnetic moment. Our theoretical results are in quantitative agreement with the experiments on the magnitude of the negative magnetoresistance. We also show the important roles played by the orbital magnetic moment and g-factors. Our results give a reasonable explanation to the negative magnetoresistance in 3D topological insulators and will be helpful in understanding the anomalous quantum transport in topological states of matter.

Introduction - Recently discovered topological semimetals are characterized by a negative magnetoresistance [1–13], which is rare in non-magnetic materials. The negative magnetoresistance is widely believed to be a signature showing that a topological semimetal can host the chiral anomaly, that is, the conservation of chiral current is violated as a result of the quantization [14–16]. However, in other systems where the chiral anomaly is not well defined, e.g., in topological insulators, a negative magnetoresistance has also been observed and has created great confusion [17–21]. In this Letter, we present a quantitative study on the magnetoresistance of 3D topological insulators. Using the semiclassical Boltzmann formalism, we explicitly take into account the correction to the conductivity from the anomalous velocity induced by the Berry curvature and orbital moment of the bulk states. By using the parameters for Bi₂Se₃, we find that the magnetoresistance can be negative when the magnetic field is applied parallel with the current. In a magnetic field up to 5 Tesla, the calculated negative magnetoresistance can be more than -1% and of the same order as those in the experiments (see Table I). The negative magnetoresistance is not sensitive to temperature, as expected by its semiclassical nature. The negative magnetoresistance depends on the Fermi energy, and its magnitude increases when approaching the band edge. We also find that the magnetoresistance depends on the signs of g-factors, and may provide an approach to measure the g-factors for these materials. Our results are consistent with those observed in the experiments, thus give a reasonable explanation to the experimentally observed negative magnetoresistance in 3D topological insulators, and will be helpful for understanding the anomalous quantum transport in topological states of matter.

Anomalous velocity - First, we illustrate that the anomalous velocity induced by the Berry curvature and its derivative orbital magnetic moment is the reason behind the negative magnetoresistance. In the experiments of topological insulators, the negative magnetoresistance can survive above $T = 100$ K [20], so quantum mechanisms, such as the weak localization effect, can be excluded. Moreover, because of the poor mobility in the topological insulators Bi₂Se₃ and Bi₂Te₃ [22], the Landau levels cannot be well-formed up to 6 Tesla in the experiments. In this semiclassical regime, the electronic transport can be described by the equations of motion [23]

$$\begin{aligned}\dot{\mathbf{r}} &= \frac{1}{\hbar} \nabla_{\mathbf{k}} \tilde{\epsilon}_{\mathbf{k}} - \dot{\mathbf{k}} \times \boldsymbol{\Omega}_{\mathbf{k}}, \\ \dot{\mathbf{k}} &= -\frac{e}{\hbar} \mathbf{E} - \frac{e}{\hbar} \dot{\mathbf{r}} \times \mathbf{B},\end{aligned}\quad (1)$$

where both the position \mathbf{r} and wave vector \mathbf{k} appear simultaneously, $\dot{\mathbf{r}}$ and $\dot{\mathbf{k}}$ are their time derivatives, $-e$ is the electron, \mathbf{E} and \mathbf{B} are external electric and magnetic fields, respectively. $\tilde{\epsilon}_{\mathbf{k}} = \epsilon_{\mathbf{k}} - \mathbf{m} \cdot \mathbf{B}$, $\epsilon_{\mathbf{k}}$ is the band dispersion, \mathbf{m} is the orbital magnetic moment induced by the semiclassical self-rotation of the Bloch wave packet, and $\boldsymbol{\Omega}_{\mathbf{k}}$ is the Berry curvature [24].

In the linear-response limit, Eq. (1) yields an effective velocity

$$\dot{\mathbf{r}} = \frac{1}{D_{\mathbf{k}}} \left[\tilde{\mathbf{v}}_{\mathbf{k}} + \frac{e}{\hbar} \mathbf{B} (\tilde{\mathbf{v}}_{\mathbf{k}} \cdot \boldsymbol{\Omega}_{\mathbf{k}}) \right], \quad (2)$$

where the group velocity of the Bloch electrons $\tilde{\mathbf{v}}_{\mathbf{k}} = \mathbf{v}_{\mathbf{k}} - \frac{1}{\hbar} \nabla_{\mathbf{k}} (\mathbf{m}_{\mathbf{k}} \cdot \mathbf{B})$ and the correction to the density of states in phase space $D_{\mathbf{k}} = 1 + \frac{e}{\hbar} \mathbf{B} \cdot \boldsymbol{\Omega}_{\mathbf{k}}$. Because of the Berry curvature, the velocity develops an anomalous term that is proportional to \mathbf{B} . Note that the conductivity is the current-current (velocity-velocity) correlation [25], thus the presence of the anomalous velocity is expected to generate an extra conductivity that

grows with the magnetic field. In other words, the Berry curvature and its derivative orbital magnetic moment may induce a negative magnetoresistance. It has been implied that the negative magnetoresistance in topological semimetals is related to the Berry curvature [26–28], which diverges near the Weyl nodes and can make a prominent contribution. The concern is whether this mechanism is large enough in topological insulators as those observed in the experiments. Experimentally the relative change in the longitudinal magnetoconductivity can exceed 1% (see Table I) when the magnetic field is a few Tesla and aligns parallel with the electric current. Later, we will use a realistic model of topological model to show that the Berry curvature can lead to a negative magnetoresistance comparable with the experiments.

Model and conductivity formula - A well accepted $k \cdot p$ Hamiltonian for 3D topological insulators can be written as [29, 30]

$$H_0 = C_{\mathbf{k}} + \begin{pmatrix} M_{\mathbf{k}} & 0 & iV_{\parallel}k_z & -iV_{\parallel}k_{-} \\ 0 & M_{\mathbf{k}} & iV_{\parallel}k_{+} & iV_{\parallel}k_z \\ -iV_{\parallel}k_z & -iV_{\parallel}k_{-} & -M_{\mathbf{k}} & 0 \\ iV_{\parallel}k_{+} & -iV_{\parallel}k_z & 0 & -M_{\mathbf{k}} \end{pmatrix} \quad (3)$$

where $M_{\mathbf{k}} = M_0 + M_{\perp}(k_x^2 + k_y^2) + M_z k_z^2$, $C_{\mathbf{k}} = C_0 + C_{\perp}(k_x^2 + k_y^2) + C_z k_z^2$, M_i , V_i , and C_i are model parameters. The model corresponds to a 3D strong topological insulator when $M_0 M_{\perp} < 0$ and $M_0 M_z < 0$ [31]. The model describes four energy bands $\varepsilon_n(\mathbf{k})$ of 3D bulk states near the Γ point, two conduction bands and two valence bands. We will assume that the Fermi level crosses only the two conduction bands. In systems with both time- and centrosymmetric symmetries, the Berry curvature vanishes at every \mathbf{k} point in the Brillouin zone, which is the case in pristine 3D topological insulators. In the presence of the magnetic field, a nonzero distribution of the Berry curvature can be induced by the Zeeman effect that breaks time reversal symmetry. The Zeeman Hamiltonian reads

$$H_Z = \frac{\mu_B}{2} \begin{pmatrix} g_z^v B_z & g_p B_{-} & 0 & 0 \\ g_p^v B_{+} & -g_z^v B_z & 0 & 0 \\ 0 & 0 & g_z^c B_z & g_p^c B_{-} \\ 0 & 0 & g_p^c B_{+} & -g_z^c B_z \end{pmatrix}, \quad (4)$$

where μ_B is the Bohr magneton and $g_{v/c,z/p}$ are Landé g -factors for valence/conduction bands along the z direction and in the $x - y$ plane, respectively. In the Boltzmann equation formalism, the longitudinal conductivity formula is found as [27]

$$\sigma_{\mu\mu} = \sigma_{\mu\mu}^{(0)} + \sigma_{\mu\mu}^{(1)} + \sigma_{\mu\mu}^{(2)}, \quad (5)$$

where

$$\sigma_{\mu\mu}^{(0)} = e^2 \tau \int \frac{d^3 \mathbf{k}}{(2\pi)^3} v^{\mu} v^{\mu} \left(-\frac{\partial \tilde{f}_0}{\partial \tilde{\varepsilon}} \right), \quad (6)$$

$$\sigma_{\mu\mu}^{(1)} = \frac{e^2}{\hbar} \tau \int \frac{d^3 \mathbf{k}}{(2\pi)^3} \left(-\frac{\partial \tilde{f}_0}{\partial \tilde{\varepsilon}} \right) \left\{ -v^{\mu} \partial^{\mu} m^{\alpha} B_{\alpha} - \partial^{\mu} m^{\alpha} B_{\alpha} v^{\mu} + e \left[(v^{\mu} B^{\mu} + B^{\mu} v^{\mu}) v^{\alpha} \Omega_{\alpha} - v^{\mu} v^{\mu} B^{\alpha} \Omega_{\alpha} \right] \right\}, \quad (7)$$

and

$$\begin{aligned} \sigma_{\mu\mu}^{(2)} = & \frac{e^2}{\hbar} \tau \int \frac{d^3 \mathbf{k}}{(2\pi)^3} \left(-\frac{\partial \tilde{f}_0}{\partial \tilde{\varepsilon}} \right) \left\{ \frac{e^2}{\hbar} [v^{\mu} v^{\mu} (B_{\gamma} \Omega^{\gamma})^2 \right. \\ & - (v^{\mu} B^{\mu} + B^{\mu} v^{\mu}) v_{\alpha} \Omega^{\alpha} B_{\gamma} \Omega^{\gamma} + B^{\mu} B^{\mu} (v_{\alpha} \Omega^{\alpha})^2] \\ & + \frac{e}{\hbar} [(v^{\mu} \partial^{\mu} m^{\alpha} B_{\alpha} + \partial^{\mu} m^{\alpha} B_{\alpha} v^{\mu}) B^{\gamma} \Omega_{\gamma} \\ & - (v^{\mu} B^{\mu} + B^{\mu} v^{\mu}) \Omega^{\alpha} \partial_{\alpha} m^{\beta} B_{\beta} \\ & - (\partial_{\mu} m_{\alpha} B^{\alpha} B^{\mu} + B^{\mu} \partial^{\mu} m_{\alpha} B^{\alpha}) v_{\beta} \Omega^{\beta}] \\ & \left. + \frac{1}{\hbar} \partial^{\mu} m_{\alpha} B^{\alpha} \partial^{\mu} m_{\gamma} B^{\gamma} \right\}, \quad (8) \end{aligned}$$

where Ω and \mathbf{m} are the Berry curvature and orbital magnetic moment, respectively, and the transport time τ is assumed to be a constant in the semiclassical limit [32].

For the n -th band of the Hamiltonian H , the ξ component of the Berry curvature vector can be found as $(\Omega_{\mathbf{k}}^n)_{\xi} = \Omega_{\mu\nu}^n \varepsilon_{\mu\nu\xi}$, where ξ, μ, ν stand for x, y, z , $\varepsilon_{\mu\nu\xi}$ is the Levi-Civita anti-symmetric tensor, and

$$\Omega_{\mu\nu}^n = -2 \sum_{n' \neq n} \frac{\text{Im} \langle n | \frac{\partial H}{\partial k_{\mu}} | n' \rangle \langle n' | \frac{\partial H}{\partial k_{\nu}} | n \rangle}{(\varepsilon_n - \varepsilon_{n'})^2}, \quad (9)$$

where $H = H_0 + H_Z$. The orbital magnetic moment \mathbf{m} can be found as

$$m_{\mu\nu}^n = -\frac{e}{\hbar} \sum_{n' \neq n} \frac{\text{Im} \langle n | \frac{\partial H}{\partial k_{\mu}} | n' \rangle \langle n' | \frac{\partial H}{\partial k_{\nu}} | n \rangle}{\varepsilon_n - \varepsilon_{n'}}. \quad (10)$$

In the experiments, the negative magnetoresistance can be found only in bulk samples which are at least several tens of nanometers thick. This implies that the negative magnetoresistance is a bulk-state effect. Because the carriers of the 3D bulk states are much more than those of the 2D surface states, we neglect the contribution of the surface states in this work.

TABLE I. The relative magnetoresistance (MR) measured in the experiments at a magnetic field of 5 Tesla and the recorded maximum value (MR_{max}).

Experiment	MR @ 5T	MR _{max}	Thickness
Ref. [17]	-0.64% @ 1.8K	-2% @ 1.8K & 8T	200nm
Ref. [18]	-0.16% @ 80K	-0.18% @ 80K & 8T	200nm
Ref. [19]	-0.5% @ 20K	-8% @ 5K & 14T	80nm
Ref. [20]	-1.4% @ 29K	-24% @ 4.2K & 28T	290nm

Negative magnetoresistance - One of the unexpected experimental results in topological insulators is the negative magnetoresistance in parallel magnetic fields (see

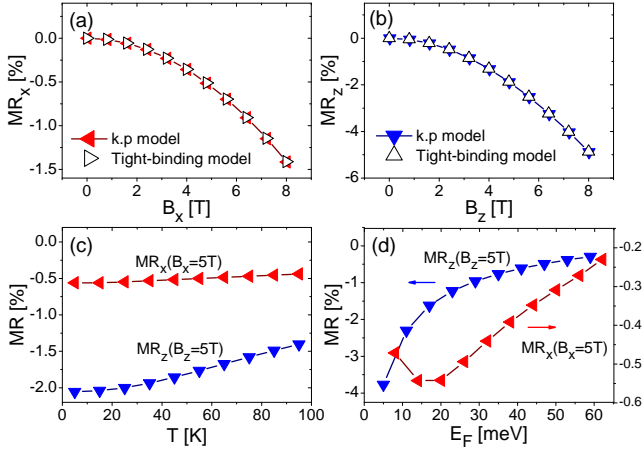


FIG. 1. The relative magnetoresistances in parallel magnetic fields. (a) $MR_x(B_x)$ and (b) $MR_z(B_z)$ at $E_F = 13$ meV and $T = 20$ K. [(c)-(d)] $MR_x(B_x = 5$ T) and $MR_z(B_z = 5$ T) as functions of temperature (c) and Fermi energy E_F (d). E_F is measured from the bottom of the conduction bands. Parameters: $M_0 = -0.169$ eV, $M_z = 3.351$ eVÅ², $M_\perp = 29.36$ eVÅ², $V_\perp = 2.512$ eVÅ, $V_n = 1.853$ eVÅ, $C_0 = 0.048$ eV, $C_z = 1.409$ eVÅ², $C_\perp = 13.9$ eVÅ² [30]. The g-factors $g_z^v = g_z^c = 30$ [33] and $g_p^v = g_p^c = -20$. No qualitative changes for the parameters from Ref. [34].

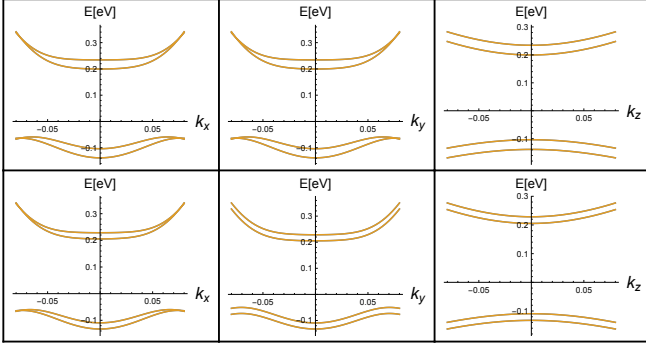


FIG. 2. The energy dispersion of the $\mathbf{k} \cdot \mathbf{p}$ model along different directions, the momenta along other two directions are set to zero. The upper panel corresponds to magnetic field in \hat{z} -direction and the lower panel is for magnetic field in \hat{x} -direction. For better demonstration, a magnetic field of 20 Tesla is used to show the Zeeman splitting of the band energies. The parameters are the same as those in Fig. 1.

Table I). In our calculation, the relative magnetoresistance is defined as

$$MR_\nu(B_\nu) = \frac{\rho_{\nu\nu}(B_\nu) - \rho_{\nu\nu}(0)}{\rho_{\nu\nu}(0)}, \quad (11)$$

where in a parallel magnetic field, say, $B_\nu = B_x$, the longitudinal resistivity $\rho_{xx} = 1/\sigma_{xx}$, and σ_{xx} is the x -direction conductivity. Figures 1(a) and 1(b) show the relative magnetoresistance in parallel magnetic fields along the x and z directions (y is equivalent to x), respectively. In both directions, the magnetoresistances are

negative and decrease monotonically with the magnetic field. The magnetic field dependence of the negative magnetoresistance can be well fitted by $-B^2$ at small magnetic fields. Within the regime of applicability of semi-classical formalism, magnetoresistance in both direction can exceed -1% , which agree *quantitatively* with the experiments. To justify our numerical results, we also use a tight-binding model [35] to perform the calculation (see [36]). The $k \cdot p$ and tight-binding models give the exactly the same results. Figure 1(c) indicates that the negative magnetoresistance is robust against raising temperature, although the magnitude is reduced. This is consistent with the experiments, showing the semi-classical nature of the negative magnetoresistance.

Figure 1(d) shows that the negative magnetoresistance becomes enhanced as the Fermi level approaches the band bottom. The magnitude of $MR_z(B_z)$ at 5 T increases monotonically with decreasing E_F . $MR_x(B_x)$ at 5 T shows a similar behavior, but with an upturn near $E_F = 13$ meV. The enhancement of the negative magnetoresistance near the band edge can be understood using Fig. 2, which shows that the Zeeman splitting is maximized at the Γ point, about several meV for a magnetic field of 5 T. The negative magnetoresistance is contributed by the Berry curvature from the two conduction bands. In the absence of the Zeeman splitting, both the Berry curvature and orbital moment vanish due to time-reversal and inversion symmetries. Because the Zeeman effect breaks time reversal symmetry, a finite distribution of the Berry curvature can be induced by the Zeeman splitting of the conduction bands. Therefore, the magnetoresistances increase with the magnitudes of Zeeman splitting and get enhanced near the band edge.

Roles of g-factors - We find that the signs of g-factors in the Zeeman coupling determine the signs of magnetoresistances *qualitatively*. Moreover, according to Eqs. (9) and (10), the signs of Ω and \mathbf{m} are controlled by the signs of g-factors, in particular $g_{z,p}^c$ when the Fermi level crosses the conduction bands. As pointed out earlier, the splitting is the largest at the Γ point, therefore the sign of the magnetoresistance is determined by the lower band with larger Fermi surface and the signs of the g-factors. We list the relation between the signs of the magnetoresistances and g-factors in Tabs. II and III. The resulting magnetoresistances differs *qualitatively* with different signs of $g_{z,p}^c$. Note that $g_{z,p}^v$ are irrelevant since we have assumed that the Fermi level crosses only the conduction bands. In the experiment, the techniques used so far for topological insulators, for example, electron spin resonance and quantum oscillations, can not determine the signs of g-factors but only their absolute values [33, 37]. Transport measurements can determine the sign of the g-factor only in specific setups [38]. Our theoretical calculation therefore provide a clue to evaluate the sign of g-factors.

Roles of orbital moment- The orbital moment has been

TABLE II. The relation between signs (\pm) of the magnetoresistances and g-factors in the z -direction magnetic field. The magnitudes g-factors are $|g_z^v| = 29.9$ and $|g_z^c| = 27.3$ [33].

g_z^v	g_z^c	$MR_{zz}(B_z)$
+	+	-
-	+	-
-	-	+
+	-	+

TABLE III. The relation between signs (\pm) of the magnetoresistances and g-factors in the x -direction magnetic field. The magnitudes g-factors are $|g_p^v| = 18.96$ and $|g_p^c| = 19.48$.

g_p^v	g_p^c	$MR_{xx}(B_x)$
-	-	-
+	-	-
+	+	+
-	+	+

neglected in most of the literature studying the magneto-transport using the semiclassical formalism [26, 27]. Both the Berry curvature and orbital moment are first-order corrections to the classical equations of motion. There is no a priori reason to exclude orbital moment at the very beginning. As shown in Ref. [39], the orbital moment is essential for a Weyl semimetal to produce the anisotropy in the magnetoconductivity. The first-order contribution Eq. (7) vanishes for the Weyl semimetal. In contrast, the first-order contributions become dominant in the present case of topological insulator. This means that the Berry curvature alone can produce an anisotropy in the magnetoconductivity. We shall emphasize that Eq. (7) conforms with Onsager relations as well. Moreover, the correction $\mathbf{m} \cdot \mathbf{B}$ to $\varepsilon(\mathbf{k})$ can enhance the band separation and the negative magnetoresistance. To see the effects of the orbital moment, Fig. 3 shows the magnetoconductivity

$$MC_\nu(B_\nu) = \frac{\sigma_{\nu\nu}(B_\nu) - \sigma_{\nu\nu}(0)}{\sigma_{\nu\nu}(0)}, \quad (12)$$

in the presence and absence of \mathbf{m} . We can see the orbital moment effectively *enhances* the magnetoresistance a few times larger. We conclude that the orbital moment is essential in producing the quantitatively correct results.

Conclusions - To conclude, we have demonstrated that the longitudinal negative magnetoresistance observed in 3D topological insulators can be understood quantitatively by the semiclassical Boltzmann equations that take into account the Berry curvature and orbital moment corrections. Our results of numerical calculations on the magnetoresistance are consistent with the experiments on the order of magnitude and temperature dependence. It is widely believed that the negative magnetoresistance

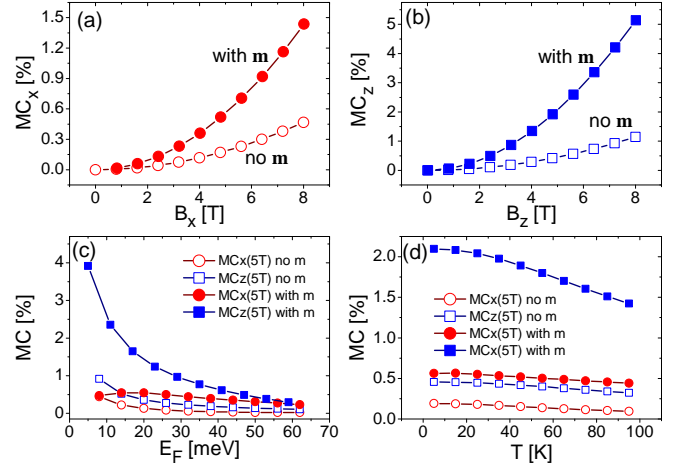


FIG. 3. The relative magnetoconductances in parallel magnetic fields. (a) $MC_x(B_x)$ and (b) $MC_z(B_z)$ at $E_F = 13$ meV and $T = 20$ K, in the presence and absence of \mathbf{m} . [(c)-(d)] $MC_x(B_x=5T)$ and $MC_z(B_z=5T)$ as functions of the Fermi energy E_F (c) and temperature (d), in the presence and absence of \mathbf{m} . The parameters are the same as those in Fig. 1.

comes with the Weyl nodes and chiral anomaly generated by the inter-node charge pumping. In topological insulators, there is no well-defined chirality, not to mention the chiral anomaly. Our results show that the negative magnetoresistance in the parallel magnetic field can happen in the absence of the chiral anomaly.

Acknowledgments - X.D. thanks the helpful discussions with Hong Yao and Pablo San-Jose. This work was supported by the National Key R & D Program (Grant No. 2016YFA0301700), National Natural Science Foundation of China (Grant Nos. 11474175 and 11574127), and the National Thousand-Young-Talents Program. Xin Dai and Z. Z. Du contribute equally to this work.

- [1] H. J. Kim, K. S. Kim, J. F. Wang, M. Sasaki, N. Satoh, A. Ohnishi, M. Kitaura, M. Yang, and L. Li, "Dirac versus Weyl fermions in topological insulators: Adler-Bell-Jackiw anomaly in transport phenomena," *Phys. Rev. Lett.* **111**, 246603 (2013).
- [2] Ki-Seok Kim, Heon-Jung Kim, and M. Sasaki, "Boltzmann equation approach to anomalous transport in a Weyl metal," *Phys. Rev. B* **89**, 195137 (2014).
- [3] Q. Li, D. E. Kharzeev, C. Zhang, Y. Huang, I. Pletikoscic, A. V. Fedorov, R. D. Zhong, J. A. Schneeloch, G. D. Gu, and T. Valla, "Chiral magnetic effect in $ZrTe_5$," *Nature Phys.* **12**, 550–554 (2016).
- [4] C. Zhang, S. Y. Xu, I. Belopolski, Z. Yuan, Z. Lin, B. Tong, N. Alidoust, C. C. Lee, S. M. Huang, T. R. Chang, H. T. Jeng, H. Lin, M. Neupane, D. S. Sanchez, H. Zheng, G. Bian, J. Wang, C. Zhang, H. Z. Lu, S. Q. Shen, T. Neupert, M. Z. Hasan, and S. Jia, "Signatures of the Adler-Bell-Jackiw chiral anomaly in a Weyl

- Fermion semimetal,” *Nat. Commun.* **7**, 10735 (2016).
- [5] X. C. Huang, L. X. Zhao, Y. J. Long, P. P. Wang, D. Chen, Z. H. Yang, H. Liang, M. Q. Xue, H. M. Weng, Z. Fang, X. Dai, and G. F. Chen, “Observation of the chiral-anomaly-induced negative magnetoresistance in 3D Weyl semimetal TaAs,” *Phys. Rev. X* **5**, 031023 (2015).
 - [6] J. Xiong, S. K. Kushwaha, T. Liang, J. W. Krizan, M. Hirschberger, W. Wang, R. J. Cava, and N. P. Ong, “Evidence for the chiral anomaly in the Dirac semimetal Na_3Bi ,” *Science* **350**, 413 (2015).
 - [7] C. Z. Li, L. X. Wang, H. W. Liu, J. Wang, Z. M. Liao, and D. P. Yu, “Giant negative magnetoresistance induced by the chiral anomaly in individual Cd_3As_2 nanowires,” *Nature Commun.* **6**, 10137 (2015).
 - [8] Cheng Zhang, Enze Zhang, Yanwen Liu, Zhi-Gang Chen, Sihang Liang, Junzhi Cao, Xiang Yuan, Lei Tang, Qian Li, Teng Gu, Yizheng Wu, Jin Zou, and Faxian Xiu, “Detection of chiral anomaly and valley transport in Dirac semimetals,” [arXiv:1504.07698](#) (2015).
 - [9] H. Li, H. T. He, H. Z. Lu, H. C. Zhang, H. C. Liu, R. Ma, Z. Y. Fan, S. Q. Shen, and J. N. Wang, “Negative magnetoresistance in Dirac semimetal Cd_3As_2 ,” *Nature Commun.* **7**, 10301 (2016).
 - [10] Frank Arnold, Chandra Shekhar, Shu-Chun Wu, Yan Sun, Ricardo Donizeth dos Reis, Nitesh Kumar, Marcel Naumann, Mukattu O. Ajeesh, Marcus Schmidt, Adolfo G. Grushin, Jens H. Bardarson, Michael Baenitz, Dmitry Sokolov, Horst Borrmann, Michael Nicklas, Claudia Felser, Elena Hassinger, and Binghai Yan, “Negative magnetoresistance without well-defined chirality in the Weyl semimetal TaP,” *Nature Commun.* **7**, 11615 (2016).
 - [11] X. J. Yang, Y. P. Liu, Z. Wang, Y. Zheng, and Z. A. Xu, “Chiral anomaly induced negative magnetoresistance in topological Weyl semimetal NbAs,” [arXiv:1506.03190](#) (2015).
 - [12] Xiaojun Yang, Yupeng Li, Zhen Wang, Yi Zhen, and Zhu-an Xu, “Observation of negative magnetoresistance and nontrivial π Berry’s phase in 3D Weyl semi-metal NbAs,” [arXiv:1506.02283](#) (2015).
 - [13] Huichao Wang, Chao-Kai Li, Haiwen Liu, Jiaqiang Yan, Junfeng Wang, Jun Liu, Ziquan Lin, Yanan Li, Yong Wang, Liang Li, David Mandrus, X. C. Xie, Ji Feng, and Jian Wang, “Chiral anomaly and ultrahigh mobility in crystalline HfTe_5 ,” *Phys. Rev. B* **93**, 165127 (2016).
 - [14] S. L. Adler, “Axial-vector vertex in spinor electrodynamics,” *Phys. Rev.* **177**, 2426–2438 (1969).
 - [15] J. S. Bell and R. Jackiw, “A PCAC puzzle: $\pi^0 \rightarrow \gamma\gamma$ in the σ -model,” *Il Nuovo Cimento A* **60**, 47–61 (1969).
 - [16] H. B. Nielsen and M. Ninomiya, “Absence of neutrinos on a lattice: (i). Proof by homotopy theory,” *Nuclear Physics B* **185**, 20 – 40 (1981).
 - [17] Jian Wang, Handong Li, Cuizu Chang, Ke He, Joon-Sue Lee, Haizhou Lu, Yi Sun, Xucun Ma, Nitin Samarth, Shunqing Shen, Qikun Xue, Maohai Xie, and Moses H.W. Chan, “Anomalous anisotropic magnetoresistance in topological insulator films,” *Nano Research* **5**, 739–746 (2012).
 - [18] H. T. He, H. C. Liu, B. K. Li, X. Guo, Z. J. Xu, M. H. Xie, and J. N. Wang, “Disorder-induced linear magnetoresistance in (221) topological insulator Bi_2Se_3 films,” *Appl. Phys. Lett.* **103**, 031606 (2013).
 - [19] Li-Xian Wang, Yuan Yan, Liang Zhang, Zhi-Min Liao, Han-Chun Wu, and Da-Peng Yu, “Zeeman effect on surface electron transport in topological insulator Bi_2Se_3 nanoribbons,” *Nanoscale* **7**, 16687–16694 (2015).
 - [20] S. Wiedmann, A. Jost, B. Fauqué, J. van Dijk, M. J. Meijer, T. Khouri, S. Pezzini, S. Grauer, S. Schreyeck, C. Brüne, H. Buhmann, L. W. Molenkamp, and N. E. Hussey, “Anisotropic and strong negative magnetoresistance in the three-dimensional topological insulator Bi_2Se_3 ,” *Phys. Rev. B* **94**, 081302 (2016).
 - [21] Oliver Breunig, Zhiwei Wang, A. A. Taskin, Jonathan Lux, Achim Rosch, and Yoichi Ando, “Gigantic negative magnetoresistance in a disordered topological insulator,” [arXiv:1703.10784](#) (2017).
 - [22] Dimitrie Culcer, “Transport in three-dimensional topological insulators: Theory and experiment,” *Physica E* **44**, 860 – 884 (2012).
 - [23] Ganesh Sundaram and Qian Niu, “Wave-packet dynamics in slowly perturbed crystals: Gradient corrections and Berry-phase effects,” *Phys. Rev. B* **59**, 14915–14925 (1999).
 - [24] D. Xiao, M. C. Chang, and Q. Niu, “Berry phase effects on electronic properties,” *Rev. Mod. Phys.* **82**, 1959–2007 (2010).
 - [25] Gerald D. Mahan, *Many-Particle Physics* (Plenum Press, 1990).
 - [26] D. T. Son and B. Z. Spivak, “Chiral anomaly and classical negative magnetoresistance of Weyl metals,” *Phys. Rev. B* **88**, 104412 (2013).
 - [27] S.-K. Yip, “Kinetic equation and magneto-conductance for Weyl metal in the clean limit,” [arXiv:1508.01010](#) (2015).
 - [28] Hai-Zhou Lu and Shun-Qing Shen, “Quantum transport in topological semimetals under magnetic fields,” *Front. Phys.* **12**, 127201 (2017).
 - [29] Haijun Zhang, Chao-Xing Liu, Xiao-Liang Qi, Xi Dai, Zhong Fang, and Shou-Cheng Zhang, “Topological insulators in Bi_2Se_3 , Bi_2Te_3 and Sb_2Te_3 with a single Dirac cone on the surface,” *Nature Phys.* **5**, 438–442 (2009).
 - [30] I. A. Nechaev and E. E. Krasovskii, “Relativistic $\mathbf{k} \cdot \mathbf{p}$ Hamiltonians for centrosymmetric topological insulators from *ab initio* wave functions,” *Phys. Rev. B* **94**, 201410 (2016).
 - [31] Shun-Qing Shen, *Topological Insulators* (Springer-Verlag, Berlin Heidelberg, 2012).
 - [32] A. A. Burkov, “Chiral anomaly and diffusive magnetotransport in Weyl metals,” *Phys. Rev. Lett.* **113**, 247203 (2014).
 - [33] A. Wolos, S. Szyszko, A. Drabinska, M. Kaminska, S. G. Strzelecka, A. Hruban, A. Materna, M. Piersa, J. Borysiuk, K. Sobczak, and M. Konczykowski, “ g -factors of conduction electrons and holes in Bi_2Se_3 three-dimensional topological insulator,” *Phys. Rev. B* **93**, 155114 (2016).
 - [34] Chao-Xing Liu, Xiao-Liang Qi, HaiJun Zhang, Xi Dai, Zhong Fang, and Shou-Cheng Zhang, “Model Hamiltonian for topological insulators,” *Phys. Rev. B* **82**, 045122 (2010).
 - [35] Shijun Mao, Ai Yamakage, and Yoshio Kuramoto, “Tight-binding model for topological insulators: Analysis of helical surface modes over the whole Brillouin zone,” *Phys. Rev. B* **84**, 115413 (2011).
 - [36] See Supplemental Materials for the detailed calculations.
 - [37] H. Köhler and E. Wöchner, “The g -factor of the conduction electrons in Bi_2Se_3 ,” *physica status solidi (b)* **67**, 665–675 (1975).

- [38] A. Srinivasan, K. L. Hudson, D. Miserev, L. A. Yeoh, O. Klochan, K. Muraki, Y. Hirayama, O. P. Sushkov, and A. R. Hamilton, “Electrical control of the sign of the g factor in a gaas hole quantum point contact,” [Phys. Rev. B **94**, 041406 \(2016\)](#).
- [39] Takahiro Morimoto, Shudan Zhong, Joseph Orenstein, and Joel E. Moore, “Semiclassical theory of nonlinear magneto-optical responses with applications to topological Dirac/Weyl semimetals,” [Phys. Rev. B **94**, 245121 \(2016\)](#).

Supplemental Material for “Negative magnetoresistance in 3D topological insulators”

Derivation of the magnetoconductivity

The expression for the electric current density can be written as

$$\mathbf{J} = -e \int \frac{d^d k}{(2\pi)^d} (D_{\mathbf{k}} \dot{\mathbf{r}} + \nabla_{\mathbf{r}} \times \mathbf{m}_{\mathbf{k}}) \tilde{\mathbf{f}}, \quad (13)$$

where $\dot{\mathbf{r}}$ is given by

$$\dot{\mathbf{r}} = \frac{1}{D_{\mathbf{k}}} \left[\tilde{\mathbf{v}}_{\mathbf{k}} + \frac{e}{\hbar} \mathbf{B} (\tilde{\mathbf{v}}_{\mathbf{k}} \cdot \boldsymbol{\Omega}_{\mathbf{k}}) \right]. \quad (14)$$

The second term is the orbital magnetic moment current and vanishes in a uniform system. We have used \tilde{f} to emphasize that the distribution function depends on $\tilde{\varepsilon}$. The distribution function can be solved from the linearized Boltzmann equation, which in the static and uniform case reads

$$\dot{\mathbf{J}} \cdot \nabla_{\mathbf{k}} \tilde{f} = \left(\frac{d\tilde{f}}{dt} \right)_{\text{collision}} = -\frac{\tilde{f} - \tilde{f}_0}{\tau}, \quad (15)$$

where in the second equality we have used the relaxation time approximation, \tilde{f}_0 is the Fermi-Dirac distribution, and the scattering time τ is treated as a constant in the small \mathbf{E} field limit.

By solving Eq. (15), we have

$$\begin{aligned} \tilde{f} - \tilde{f}_0 &= \frac{e\tau}{\hbar^2 D_{\mathbf{k}}} [\hbar \mathbf{E} + e(\mathbf{E} \cdot \mathbf{B}) \boldsymbol{\Omega}] \cdot \nabla_{\mathbf{k}} \tilde{f} \\ &= \frac{e\tau}{\hbar D_{\mathbf{k}}} [\hbar \mathbf{E} + e(\mathbf{E} \cdot \mathbf{B}) \boldsymbol{\Omega}] \cdot \tilde{\mathbf{v}} \left(-\frac{\partial \tilde{f}_0}{\partial \tilde{\varepsilon}} \right). \end{aligned} \quad (16)$$

By putting Eq. (16) into Eq. (13), in the linear response regime we have

$$\begin{aligned} J^\mu &= e^2 \tau \int \frac{d^3 k}{(2\pi)^3} D_{\mathbf{k}}^{-1} \left(\tilde{v}^\mu + \frac{e}{\hbar} B^\mu \tilde{v}_\alpha \Omega_{\mathbf{k}}^\alpha \right) \\ &\quad \times \left(E^\nu + \frac{e}{\hbar} E^\beta B_\beta \Omega_{\mathbf{k}}^\nu \right) \tilde{v}_\nu \left(-\frac{\partial \tilde{f}_0}{\partial \tilde{\varepsilon}} \right). \end{aligned} \quad (17)$$

The conductivity tensor is therefore

$$\begin{aligned} \sigma^{\mu\nu} &= e^2 \tau \int \frac{d^3 k}{(2\pi)^3} D_{\mathbf{k}}^{-1} \left(\tilde{v}^\mu + \frac{e}{\hbar} B^\mu \tilde{v}_\alpha \Omega_{\mathbf{k}}^\alpha \right) \\ &\quad \times \left(\tilde{v}^\nu + \frac{e}{\hbar} B^\nu \tilde{v}_\beta \Omega_{\mathbf{k}}^\beta \right) \left(-\frac{\partial \tilde{f}_0}{\partial \tilde{\varepsilon}} \right). \end{aligned} \quad (18)$$

The Einstein summation convention is assumed. In the small magnetic field limit, $D_{\mathbf{k}}^{-1}$ can be expanded as

$$D_{\mathbf{k}}^{-1} \simeq 1 - \frac{e}{\hbar} \mathbf{B} \cdot \boldsymbol{\Omega}_{\mathbf{k}} + \frac{e^2}{\hbar^2} (\mathbf{B} \cdot \boldsymbol{\Omega}_{\mathbf{k}})^2, \quad (19)$$

then we arrive at the results of $\sigma_{\mu\mu}^{(0)}$, $\sigma_{\mu\mu}^{(1)}$, and $\sigma_{\mu\mu}^{(2)}$ in the main text. The three terms are not exactly classified according to the order of B , because $-\partial \tilde{f}_0 / \partial \tilde{\varepsilon}$ also depends on \mathbf{B} . In a work on Weyl semimetals, $-\partial \tilde{f}_0 / \partial \tilde{\varepsilon}$ was also expanded in \mathbf{B} [39]. We express the conductivity in a more compact form, which facilitates the numerical calculations.

Benchmark with tight-binding model

The tight-binding model used in the benchmark was proposed in Ref. [35]. The convergence of two models is expected since the tight-binding model reduces to the continuum model as the fermi surface shrinks down to Γ point. The details of the tight-binding model can be found in Ref. [35]. Here we just give the relevant analytical expressions,

$$H(\mathbf{k}) = h_0 + h_1 \sigma_x \tau_x + h_2 \sigma_y \tau_x + h_3 \sigma_z \tau_x + h_4 \sigma_0 \tau_y + h_5 \sigma_0 \tau_z, \quad (20)$$

where

$$h_0 = 2A_0 \sum_i^3 \cos k_{ai} + 2B_0 \sum_{i=1}^3 \cos k_{bi}, \quad (21)$$

$$h_1 = -2A_{14} \sin \omega [\sin k_{a2} - \sin k_{a3}], \quad (22)$$

$$h_2 = -2B_{14} \sin \omega (\sin k_{b2} - \sin k_{b3}), \quad (23)$$

$$h_3 = 2A_{12} \sum_{i=1}^3 \sin k_{ai}, \quad (24)$$

$$h_4 = -2B_{12} \sum_{i=1}^3 \sin k_{bi},$$

$$h_5 = 2A_{11} \sum_{i=1}^3 \cos k_{ai} + 2B_{11} \sum_{i=1}^3 \cos k_{bi} + m_{11}, \quad (25)$$

where $\omega = -2\pi/3$, $k_{ai} \equiv \mathbf{k} \cdot \mathbf{a}_i$ and $k_{bi} \equiv \mathbf{k} \cdot \mathbf{b}_i$.

It can be seen immediately that Eq. (20) reduces to the $k \cdot p$ Hamiltonian near the Γ point, up to a basis transformation. The parameters used in both models are related as

$$\begin{aligned} c_z &= -3B_0, \quad \frac{3}{2}A_0 + \frac{1}{2}B_0 = -c_\perp, \\ M_z &= -3B_{11}, \quad M_0 = 6(A_{11} + B_{11}) + m_{11}, \\ M_\perp &= -(\frac{3}{2}A_{11} + \frac{1}{2}B_{11}), \quad V_n = 3A_{14} + \sqrt{3}B_{14}. \end{aligned} \quad (26)$$

Note that A_{14} , B_{14} and A_{12} are not uniquely determined. Nevertheless their numerical values do not affect the transport results. We have also set $a = c = 1$ for simplicity.